



Contents lists available at ScienceDirect

Journal of Neuroscience Methods

journal homepage: www.elsevier.com/locate/jneumeth



Quantifying chirp in sleep spindles

Suzana V. Schönwald^{a,*}, Diego Z. Carvalho^a, Guilherme Dellagustin^a,
Emerson L. de Santa-Helena^b, Günther J.L. Gerhardt^c

^a Neurology Section, Hospital de Clínicas de Porto Alegre, Rua Ramiro Barcelos 2350/sala 2040/90035-003 Porto Alegre, RS, Brazil

^b Departamento de Física, Universidade Federal do Sergipe, Aracaju, SE, Brazil

^c Departamento de Física e Química da Universidade de Caxias do Sul, Rua Francisco Getulio Vargas 1130, 95001-970 Caxias do Sul, RS, Brazil

ARTICLE INFO

Article history:

Received 21 October 2010
Received in revised form 20 January 2011
Accepted 21 January 2011

PACS:

87.19La
87.19Vn
06.30.Ft
07.05.Rm

Keywords:

Time series
Matching pursuit
EEG
Sleep spindles
Spectral analysis
Chirp

ABSTRACT

Sleep spindles are considered as a marker of integrity for thalamo-cortical circuits. Recently, attention has been given to internal frequency variation in sleep spindles. In this study, a procedure based on matching pursuit with a Gabor-chirplet dictionary was applied in order to measure chirp rate in atoms representing sleep spindles, also categorized into negative, positive or zero chirp types. The sample comprised 707 EEG segments containing visual sleep spindles, labeled TP, obtained from nine healthy male volunteers (aged 20–34, average 24.6 y). Control datasets were 333 non-REM (NREM) sleep background segments and 287 REM sleep intervals, each with 16 s duration. Analyses were carried out on the C3-A2 EEG channel. In TP and NREM groups, the proportion of non-null chirp types was non-random and total chirp distribution was asymmetrical towards negative values, in contrast to REM. Median negative chirp rate in the TP and NREM groups was significantly lower than in REM (-0.4 Hz/s vs -0.3 Hz/s, $P < 0.05$). Negative chirp atoms outnumbered positives by 50% in TP, while in NREM and REM, they were, respectively, only 22% and 12% more prevalent. TP negative chirp atoms were significantly higher in amplitude compared to positive or zero types. Considering individual subjects, 88.9% had a TP negative/positive chirp ratio above 1 (mean \pm sd = 1.64 ± 0.65). We propose there is increasing evidence, corroborated by the present study, favoring systematic measurement of sleep spindle chirp rate or internal frequency variation. Preferential occurrence of negatively chirping spindles is consistent with the hypothesis of electrophysiological modulation of neocortical memory consolidation.

© 2011 Elsevier B.V. All rights reserved.

1. Introduction

The sleep EEG signal contains an enormous wealth of detail, and a lack of stationarity nearly as significant (Lopes da Silva, 2005a). Conventionally, sleep EEG transients are described in terms of their representation in the time \times voltage domain. The best studied sleep EEG transient, the sleep spindle, is defined as waxing and waning wave trains with characteristic morphology, frequency ranging from 11 Hz to 16 Hz (most commonly, 12 Hz–14 Hz), duration equal to or greater than 0.5 s (in average, less than 2 s) and maximal voltage in central EEG derivations (Rechtschaffen and Kales, 1968; Jankel and Niedermeyer, 1985; Iber et al., 2007). Spindles occur in hundreds to thousands within NREM sleep; “waxing and waning” implies non-stationarity even within their own short time frame. Sleep spindles are reportedly modified in the context of brain pathology; they are considered to be a marker of integrity for thalamo-cortical circuits, and have recently been

incorporated into models of memory consolidation and amplifying mechanisms (Born and Rasch, 2006). In model diagrams for the sleep spindle origin (Destexhe et al., 1994; Destexhe and Sejnowski TJ, 2009; Steriade, 2000), neurons from the thalamic reticulum (RE) induce firing in thalamo-cortical (TC) neurons, generating spindle oscillations that can be ultimately measured over the scalp. This thalamo-cortical/thalamic reticulum (TC-RE) network rhythmicity is related to excitatory and inhibitory mechanisms linked to local changes in ion currents (Steriade, 2000).

Spindles detected over the scalp display a spectral “chirp” or shear effect that can be measured in a train of discharges. In other words, the firing sequence can accelerate, decelerate or maintain a stable frequency over time (Dehgani et al., 2011). This effect is possibly too subtle to be reliably discriminated visually. Recently, however, these transients have been subjected to spectral decomposition and quantitative analysis with a variety of techniques, including representation on a time \times frequency plane related to voltage (Fig. 1). Fine frequency modulation over a short time span becomes thus readily visible and has been verified for single epidurally recorded frontal sleep spindles in rats (Sitnikova et al., 2009). Spindle frequency modulation has been studied in simulated signals, modeled, tested in a limited sample of 22 spindles

* Corresponding author. Tel.: +55 51 9641 4740; fax: +55 51 3312 2725.
E-mail addresses: sschonwald@hcpa.ufrgs.br (S.V. Schönwald),
gunther.lew@yahoo.com.br (G.J.L. Gerhardt).

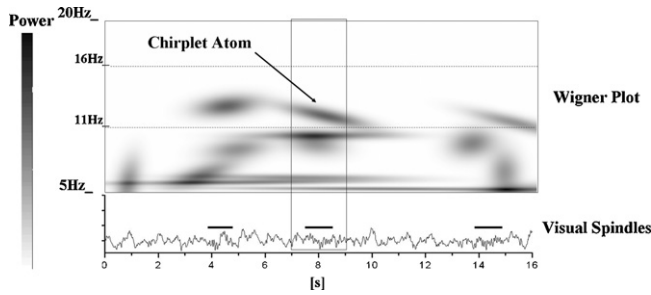


Fig. 1. Example of EEG signal reconstruction showing internal sleep spindle frequency modulation in the True Positives dataset, as represented by chirplet atoms. Below, 16 s EEG window with three visually selected sleep spindles. Above, signal spectral decomposition in terms of Gabor chirplet atoms in a Wigner plot. The procedure is exemplified for visual spindle 2. The visual spindle is positioned in the center of a 16 s window and spectral decomposition is carried out; atoms fulfilling the selection criteria and appearing within a 1s-margin of the window center are collected for analysis; the procedure is repeated for each visual spindle scored. Notice important contribution from slower frequencies. Only the most significant atoms are shown for clarity.

and found to be different between dementia patients and elderly controls (Ktonas et al., 2009). Because these oscillations reflect thalamo-cortical activity, their internal frequency variation may bear relevant information in the context of neurophysiology as well as brain pathology investigation. However, due to the intrinsic non-stationarity of the EEG signal, even if a chirp effect can be verified for sleep spindles, it could still be occurring at random. Fundamental hypotheses to be tested would therefore be whether spindle chirp distribution is (a) non-random and (b) distinguishable from that obtained assessing non-spindle EEG signals.

We hereby present for the first time the application of matching pursuit (MP) with Gabor chirplet dictionary (set of functions) for the systematic measurement of human sleep spindle chirp rate. Chirplet functions and transforms have been introduced in order to deal with rapid changes of frequency that often characterize signals in nature (Baraniuk et al., 1993; Gribonval, 2001; Mann and Haykin, 1995; Yin et al., 2002). The use of MP in sleep analysis is well known (Lopes da Silva, 2005b), and MP resolution is considered suitable for sleep spindle description (Durka et al., 2001, 2002; Huupponen et al., 2007; Ktonas et al., 2009). Here the procedure described in (Durka et al., 2001) was modified in order to include a chirplet function, using the *ridge pursuit* approach proposed by (Gribonval, 2001). Matching pursuit with chirplet atoms (with different methodology) has been previously applied to the analysis of visual evoked potentials in humans (Cui et al., 2004). In the present study, chirp rate is quantified in MP atoms representing sleep spindles. It is shown that human sleep spindles contain a significant proportion of high voltage, negatively chirping elements.

2. Methods

2.1. Matching pursuit procedure with Gabor function dictionary

Matching pursuit is not a transform, it is an adaptive approximation of the signal. MP decomposes the signal by successive approximations into a linear expansion of waveforms that belong to a redundant dictionary of functions (called atoms), that are the dilations, translations and modulations of a single window function (Mallat and Zhang, 1993). In the MP approach, a signal $S(t)$ is taken and subsequent adaptation steps are made writing $S(t)$ in terms of $D = \{g_{\gamma_i}\}$

$$S(t) \simeq \sum_{i=1}^M a_i g_{\gamma_i}, \quad (1)$$

where γ_i represents a set of parameters that characterize the dictionary functions, M is the number of steps and a_i is an amplitude term which may be incorporated to g without loss of generality. For a signal of size N , $D = \{g_{\gamma_i}\}$ is a redundant dictionary of $i > N$ elements which will include at least N linearly independent vectors.

As an adaptive filter, the MP procedure matches the signal with a function g_{γ_i} at each step i , leaving a residue $RS(t)_{i+1}$ to be matched by the same procedure in step $i + 1$. Indeed, MP projects $S(t)$ on a vector g_{γ} and evaluates the residual $RS(t)_1$:

$$S(t) = \langle S(t), g_{\gamma} \rangle g_{\gamma} + RS(t)_1. \quad (2)$$

If one takes g_{γ} to be an orthogonal basis, one can write

$$\|S(t)\|^2 = |\langle S(t), g_{\gamma} \rangle|^2 + \|RS(t)_1\|^2. \quad (3)$$

In order to minimize $\|RS(t)_1\|$, g_{γ} is chosen such that $|\langle S(t), g_{\gamma} \rangle|$ is maximal or at least suboptimal. The procedure is continued iteratively replacing $RS(t)$ for the original $S(t)$ until some energy threshold or number of iterations coefficient is reached. Generalizing the procedure:

$$RS(t)_i = \langle RS(t)_i, g_{\gamma} \rangle g_{\gamma} + RS(t)_{i+1}, \quad (4)$$

for $0 < i < M$ where $RS(t)_0 \equiv S(t)$.

The original signal is thus decomposed into waveforms that can be represented as atoms in a time–frequency plane (Wigner plane). If a structure does not correlate well with any particular dictionary element, decomposition will result into several elements and information will be diluted. MP is described in detail elsewhere (Mallat and Zhang, 1993; Mallat, 1999).

The program used in this study was obtained from <http://eeg.pl> (Durka et al., 2001). The dictionary used for time–frequency analysis in this particular algorithm is built from Gabor functions and adds a set of Dirac’s delta and Fourier functions in order to deal with time and frequency well-localized structures. Gabor wavelets (sine-modulated Gaussian functions) are chosen for EEG microstructure description because they provide optimal joint time–frequency localization with a small number of parameters to be determined (as amplitude, time position, central frequency and phase) (Durka and Blinowska, 1996; Durka et al., 2001).

2.2. Matching pursuit with Gabor chirplet dictionary

Chirplets are generalizations of wavelets related to each other by two-dimensional affine coordinate transformations (translations, dilations, rotations and shears) in the time–frequency plane, as opposed to wavelets, which are related to each other by one-dimensional affine coordinate transformations (translations and dilations) in the time domain only (Mann and Haykin, 1995).

In the Gaussian chirplet function

$$g_{\gamma}(t) = \alpha e^{-\pi \left[\frac{(t-t')}{s} \right]^2} \sin \left[\frac{2\pi\omega[(t-t') + \beta(t-t')^2]}{N} + \phi \right], \quad (5)$$

N is the size of the signal, the set $\gamma = \{\alpha, t', w, s, \beta, \phi\}$ represents parameters of dictionary functions and α is chosen such that $|g_{\gamma}| = 1$ (Mann and Haykin, 1995). Actually, Gabor functions as used in (Durka et al., 2001) are a particular case of (5) where the chirping (shear) parameter $\beta = 0$.

A problem of working with functions like (5) is that they do not form an orthonormal basis and are not even linearly independent (Yin et al., 2002). Indeed, an orthonormal basis of chirp atoms is presented in (Baraniuk et al., 1993), but those functions may be “too rigid” for the treatment of some particular problems, especially concerning signals of biological nature, due to parameter dependency: $\omega \propto 1/s$ and $\beta \propto 1/s^2$ (Gribonval, 2001). Conversely, the Gaussian chirplet has no such “rigidity” but is very redundant. As redundancy significantly increases computational processing cost,

different approaches have been developed to deal with this issue (Yin et al., 2002; Cui et al., 2004; Talakoub et al., 2010). One way to deal with the problem is to employ a procedure like the ridge pursuit proposed by (Gribonval, 2001). When a scheme like MP is applied to signals of biological nature, the reconstruction will often show dominance by a few strong terms (higher amplitude atoms), while the residue may be seen as noise (Yin et al., 2002). In the *ridge pursuit* procedure, the best Gabor atom (without chirp, $\beta=0$) is initially found in the iteration; then it is explored whether an atom with a chirp parameter different from zero can better fit the signal (this procedure may represent a better signal description if local frequency variability is significant). If a chirp element (atom) fulfills the condition, this element is chosen, the residue is calculated and the procedure continues. If no chirp parameter results in a better fitting, zero chirp is chosen and the procedure continues to the next step. The ridge pursuit procedure is particularly conservative with respect to the β factor. Considering a highly non-stationary signal, it is difficult to expect an absence of chirping, but if no chirp preference occurs in the signal, MP with a procedure like ridge pursuit will expectedly yield a statistically equal proportion of positive and negative β .

In this study, the MP source code as presented in <http://eeg.pl> was modified in order to include a subroutine, whereby the two-step ridge pursuit procedure (Gribonval, 2001) was implemented using a set of functions like (5). Performance (sensitivity and specificity) of the modified code was tested for automatic spindle detection against that of the original algorithm (Durka et al., 2001), using an approach identical to what was described in (Schönwald et al., 2006), and found to be similar to the original algorithm performance. The modified code is available from authors upon request.

2.3. EEG sample

This study makes use of a sample of 6.2 h proportionally representative of human sleep, obtained from nine healthy male volunteers (aged 20–34, average 24.6 y). The sample was used in previous works where it was described in better detail (Schönwald et al., 2003, 2006). Briefly, all polysomnograms were performed in an 18-channel analog NIHON-KOHDEN polygraph with 12 bit digital conversion (STELLATE RHYTHM V10.0), recorded with 128 Hz resolution, with a 0.5 Hz high-pass filter provided by the manufacturer, 0.3 s time constant and -3 dB IIR32 digital filter conditions applied to the signal. Bipolar non-reformatable EEG leads included C3–A2, C4–A1, Fp1–T3, T3–O1, Fp2–T4 and T4–O2. Sleep was visually scored according to RK (Rechtschaffen and Kales, 1968). From a screen display of C3–A2 channel, two specialists scored all concordant spindles, hereby called visual spindles (VS), using the RK68 spindle definition. Visual spindle duration (onset and offset points) was taken from the numerical conversion (ASCII) of digital recordings by the EEG viewer employed (RHYTHM V10.0). The sample thus obtained contains 707 VS, being 513 from sleep stage 2 (S2) and 194 from sleep stages 3 (S3) and 4 (S4) (18 spindles visually detected within REM sleep were not included in this analysis and those segments were disregarded). Visual Spindle prevalence (ratio between spindle time and sleep time) was 2.38%.

A set of 707 16 s windows was then obtained from the original EEG time series, with each visual spindle, regardless of its duration, located at the window center. This dataset was subjected to signal reconstruction (see next section) and labeled true positives (TP).

Two control datasets were used in the study. The first comprises all S2, S3 and S4 sleep segments with 16 s duration or longer, where no spindles were visually detected (NREM sleep background segments, labeled NREM). There were 333 such segments in the sample. The MP signal reconstruction is *a priori* expected to obtain elements fulfilling automatic spindle detection criteria from these segments (see next subsection for details). The second control

dataset is comprised 287 16 s REM sleep intervals. These were labeled REM. REM sleep has very broad spectral composition, with no peaks expected in the sigma (11–16 Hz) frequency range.

2.4. Signal analysis procedure

All analyses were carried out on the C3–A2 EEG channel. Each 16 s EEG window was subjected to MP with Gabor chirplet dictionary stopping at 96 iterations. A dictionary size of 10^6 Gabor chirplet atoms was used. Each atom obtained with MP has a central point both in time and frequency and limits established by a half-width (HW) corresponding to $\pm\sigma$ on a gaussian curve. Atoms with HW duration between 0.5 s and 2 s, central frequency between 11 Hz and 16 Hz and chirp rate from -2 Hz/s to 2 Hz/s were filtered and collected in the procedure. In the TP dataset, only atoms appearing within a 1 s-margin from the window center were included in the analysis (Fig. 1). Chirp rate threshold was arbitrated in ± 2 Hz/s for two reasons. Firstly, frequency difference between slow and fast scalp spindles is in average below 2 Hz (Jankel and Niedermeyer, 1985; Werth et al., 1997; Anderer et al., 2001; De Gennaro and Ferrara, 2003; Huupponen et al., 2008). Secondly, short elements with chirp rate beyond this range were rare in the dataset (<1%) and associated with signal inhomogeneity.

Due to the exploratory nature of the study, no voltage amplitude threshold (AT parameter in MP) was applied. This is justified by the fact that there is still debate over an optimal voltage threshold for automatic spindle detection (Huupponen et al., 2000; Bodisz et al., 2009; Ray et al., 2010). Therefore, the NREM background atom dataset is assumed to represent a mixture of activities in the sigma frequency range, including elements that might correspond to false positive spindle detections when one considers the visual criterion as the gold standard. It should also be born in mind that AT values express a ratio, so that correspondence to signal voltage is not straightforward.

2.5. Additional statistical analysis

After signal reconstruction, data (chirp rate, atom duration, amplitude and central frequency variables) were inspected and found to have non-normal distributions (D'Agostino & Pearson omnibus normality test). Descriptive values are given as median (interquartile range). The Kruskal–Wallis analysis of variance test followed by Dunn's post-hoc pairwise comparisons was used for group comparisons. Spearman's rank correlation was used to determine the relationship between atom chirp rate and duration, amplitude and central frequency variation. Elements (atoms) were also categorized into negative, positive and zero (Null) chirp types. A binomial test was used to verify probability of random chirp category distribution (negative or positive) within each group. Prevalence of different chirp types in TP, NREM and REM groups was compared by means of the Chi-square test for categorical variables. Statistical significance was assumed for two-tailed p -value < 0.05 . Analyses were carried out with SPSS V.17 for Windows (SPSS Inc., Chicago, IL, USA) and GraphPad Prism V5.01 (San Diego, CA, USA) software packages.

3. Results

A total of 984 elements were obtained for TP, 813 for NREM and 692 for REM groups. Prevalence of negative, positive and zero chirp types was significantly different among groups (Fig. 2A) (Pearson Chi-square = 19,547; df 4; $p=0.001$). The 0 Hz/s modal peak was significantly lower in TP (17.1%) and NREM (18.0%) groups in comparison to REM (23.4%) group (Pearson Chi-square = 11,611; df 2; $p=0.003$). Considering only negative and positive chirp types, probability of random chirp categorization was significantly low

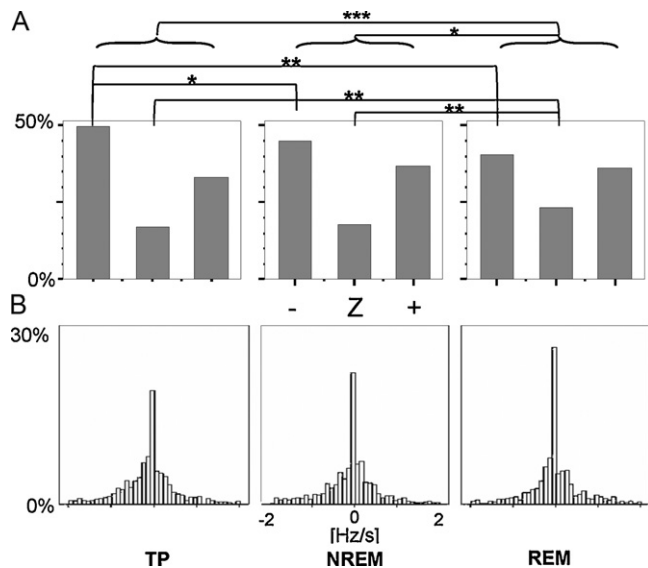


Fig. 2. (A) Proportions of negative, zero and positive chirp categories in the three groups studied showing significantly higher proportion of negatively chirping elements in the TP group. Significant Pearson Chi-square values are marked as follows: * $p < 0.05$, ** $p < 0.01$, *** $p < 0.001$. B) Total chirp rate distribution in the three groups studied. Chirp rate distribution was asymmetrical towards more negative values in the TP and NREM groups, but not in REM. TP=true positives, NREM=NREM background, REM = REM sleep, -=negative, Z=zero, +=positive.

in TP ($P < 0.001$) and NREM ($p = 0.011$) groups, but not in REM ($p = 0.208$). There was a significantly higher proportion of negative chirp elements in the TP sample (60.2%) in comparison to the NREM (55.0%) and REM (52.8%) groups (Pearson Chi-square = 7973; $df 2$; $p = 0.0019$). In other words, negative chirp atoms outnumbered positives by 50% in TP, while in NREM and REM, they were, respectively, only 22% and 12% more prevalent. Considering individual subjects, TP negative/positive chirp ratio ranged between 0.8 and 3 (mean ratio = 1.64; $sd = 0.65$), and eight of nine subjects (88.9%) had TP negative/positive chirp ratio above 1.

Chirp rate distribution (Fig. 2B), as well as conventional sleep transient descriptors (voltage amplitude, duration and central frequency) are shown in Table 1 and differed among TP, NREM and REM groups. Median negative chirp rate in the TP group, as well as in the NREM group, was significantly lower than in the REM group, while median positive chirp rate was similar for the three studied groups, with a trend towards higher values in REM. Chirp rate distribution was thus asymmetrical towards more negative values in the TP and NREM groups, but not in REM (see also Fig. 3). Compared to TP elements, NREM elements were lower in amplitude

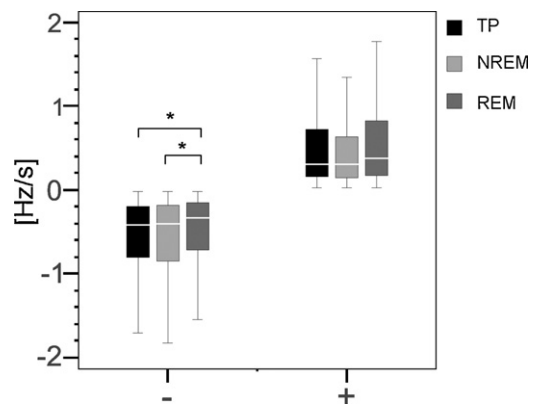


Fig. 3. Negative and positive chirp rate distribution in the three groups studied. Median negative chirp rate in the TP and NREM groups was significantly lower than in REM (-0.4 Hz/s vs -0.3 Hz/s). * $p < 0.05$ in Kruskal–Wallis test with Dunn’s post-hoc pairwise comparisons. TP=true positives, NREM=NREM background, REM = REM sleep. Box plot horizontal lines denote extreme values.

and slower in frequency, with a statistically non-significant trend towards shorter duration. In contrast, REM elements were lowest in amplitude, intermediate in frequency with the widest variation, and longest in duration (see also Fig. 4).

Fig. 4 shows atom amplitude, duration and central frequency variation according to chirp category (negative, positive or zero) within each sample. Negative chirp atoms were significantly higher in amplitude compared to positive or zero chirps in the TP sample ($H = 35.9$; $df 2$; $p < 0.0001$). Similar tendency was found within the NREM sample, with negative and positive elements significantly higher in amplitude compared to Zero chirps ($H = 28.34$; $df 2$; $p < 0.0001$). Correlation between TP negative chirp rate and voltage was weak ($r_s = -0.1689$; $p < 0.001$). No significant category effects were found for amplitude variation within the REM sample, nor concerning duration or central frequency distribution in the three groups studied. Chirp rate was moderately correlated with atom duration in all groups studied (r_s values between 0.409 and 0.503 for negatively chirping atoms, and between -0.477 and -0.555 for positively chirping atoms; all p values < 0.001).

4. Discussion

In this study, matching pursuit with a Gabor chirplet dictionary was successfully applied to the detection and measurement of spectral chirps in human sleep spindles. Chirp rate distribution was non-random; the proportion of negative, positive and zero chirp atoms significantly differed from that obtained for control datasets of similar frequency range. A significantly higher propor-

Table 1
Chirp rate, amplitude, duration and central frequency distribution in TP, NREM and REM.

	TP	NREM	REM	H	df	p-Value
Chirp rate (Hz/s)						
Total ^A	-0.2 (0.8) ^c	-0.1 (0.8)	-0.1 (0.7)	14.28	2	0.0008
Negative	-0.4 (0.6) ^d	-0.4 (0.7) ^a	-0.3 (0.6) ^a	8.872	2	0.0118
Positive	0.3 (0.6)	0.3 (0.5)	0.4 (0.7)	4.387	2	0.1115
Amplitude (μV^2)	87.58 (70.13) ^{c,c}	60.09 (39.89) ^c	35.80 (17.74)	922.2	2	<0.0001
Duration (s)	1.09 (0.68) ^b	1.04 (0.63) ^b	1.14 (0.74)	12.3	2	0.0021
Frequency (Hz)	13.3 (1.7) ^c	12.8 (1.7) ^c	13.1 (2.7)	20.38	2	<0.0001

Values expressed as median (interquartile range).

^A Total = (neg + pos) chirp rate; significant Kruskal–Wallis test with Dunn’s post-hoc pairwise comparisons marked as follows:

^a $p < 0.05$ for contiguous groups.

^b $p < 0.01$ for contiguous groups.

^c $p < 0.001$ for contiguous groups

^d $p < 0.05$ in comparisons between the first and the last group.

^e $p < 0.01$ in comparisons between the first and the last group.

^f $p < 0.001$ in comparisons between the first and the last group.

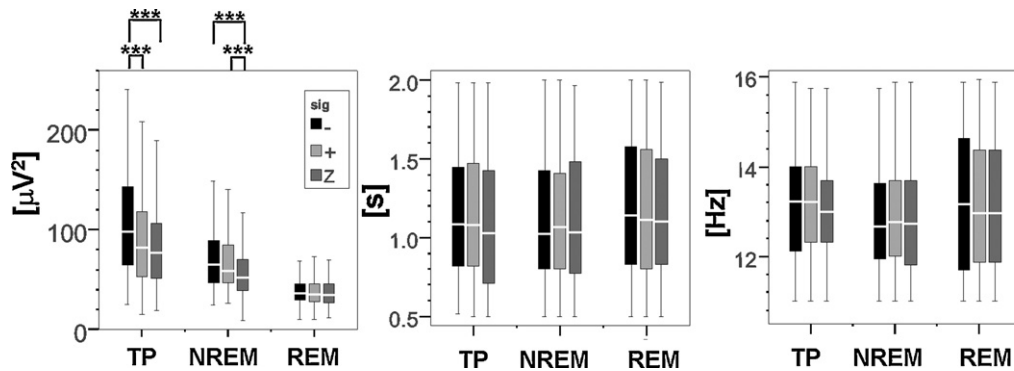


Fig. 4. Amplitude, duration and central frequency variation according to MP with Gabor chirp atom category (negative, positive or zero) in the three groups studied. TP negative chirp atoms were significantly higher in amplitude compared to positive or zero types. $***p < 0.0001$ in Kruskal–Wallis test with Dunn’s post-hoc pairwise comparisons. TP = true positives, NREM = NREM background, REM = REM sleep. Box plot horizontal lines denote extreme values.

tion of negatively chirping atoms was obtained within the sleep spindle sample. Indeed, prevalence of negative over positive chirp atoms was 50% higher in TP, compared to 22% in NREM and 12% in REM. Overall, characteristics of spindle chirp rate distribution showed some similarities to those obtained for NREM background elements, while being significantly different from those obtained for REM sleep EEG signals. This is not unexpected, considering that NREM background EEG contains some degree of information similar to that of visually detected sleep spindles, which accounts for the presence of so-called false positives in automatic spindle detection; in contrast, mechanisms responsible for spindle generation appear to be strongly inhibited during REM sleep (Steriade, 2005). The main distinctions between True Positive and NREM background features in this sample were (a) higher central frequency, (b) a trend towards longer duration and (c) higher voltage, especially for negatively chirping atoms. It thus appears that what humans recognize as true sleep spindles contains a significant proportion of high voltage, negatively chirping elements (spindle oscillations which are faster at their beginning and slower towards their end).

These results are in line with recent findings indicating that for scalp-detected sleep spindles, the most common temporospatial frequency evolution is a decline in high frequency power and increase in low frequency power from early to late in a single spindle, in association with power shift from more posterior to more anterior regions (Dehgani et al., 2011). In that study, spectral power from visually detected spindles was calculated as the average 10–16 Hz squared Morlet transform power; spindles were divided into early and late parts, and power at 12 Hz and 14 Hz was arbitrated to characterize low and high frequency energy. To the best of our knowledge, the present study is the first reporting a systematic analysis of a putatively individual sleep spindle chirp rate. Sleep spindles have been formerly reported to lack chirps (Schiff et al., 2000). However, in that study, spectral chirps with a very distinctive pattern were recognized in brain signals during focal epileptic seizures, consisting of multilayered, rapid frequency declines often spanning 10 Hz and 10–15 s windows (Schiff et al., 2000; Molaee-Ardekani et al., 2010). Human sleep spindles are much shorter in duration, and expressed over a narrower frequency band, so here a more subtle chirp effect is being considered.

Preferential occurrence of negatively chirping spindles draws attention to mechanisms initiating and terminating the spindle sequence and may have several implications. In the first place, results from current theoretical and computational models for sleep spindle generation closely approximate data obtained experimentally, except for assuming these transients to oscillate with stable internal frequency (Destexhe et al., 1994; Destexhe and Sejnowski TJ, 2009; Steriade, 2000). Possibly, the inclusion of an internal frequency variation factor would further approximate the

output from these models to experimental data. Secondly, the inclusion of a probability term relative to the differential prevalence of negative, positive and non-chirping elements might help improve automatic spindle detection algorithms. The expected benefit from such an approach, however, might be currently unworthy of the computational cost involved. More interestingly, the chirping effect may be related to neurophysiological processes modulating thalamic reticular sleep spindling in the context of memory consolidation. Declarative memory consolidation during sleep has been linked to repetitive reactivation of newly-encoded information, in connection with sharp wave-ripple (ultra-fast) activity in the hippocampus (Buzsáki, 1998). Conceptually, slow oscillations originated in neocortical networks help synchronize hippocampal memory reactivation with the occurrence of sleep spindles, ultimately leading to selective long-term plastic changes in neocortical synapses (preferentially those that were used during encoding) (Born and Rasch, 2006). In a recent study, relationship between spindle activity and procedural memory consolidation was investigated in a group of subjects trained on a motor-skill task using their left hand (Nishida and Walker, 2007). Significant correlations between memory improvement and spindle density were detected when spindle activity at the central scalp position on the non-learning (left) hemisphere was subtracted from that obtained from the learning (right) hemisphere, an effect assumed to represent a homeostatic difference following learning (Nishida and Walker, 2007). As depicted in their Fig. 4, while the averaged 12–16 Hz spectral power with 1-s duration corresponding to sleep spindles over the non-learning (left) and learning (right) central scalp positions maintained a stable frequency over time, the averaged spectral power of the difference between those two locations showed a deceleration (negative chirp) towards the second half (end) of the period. It is thus possible to hypothesize that negatively chirping spindles occur preferentially in association with specific memory consolidation processes.

The present study was limited to information available from EEG derivation C3–A2, which is assumed to represent a mixture of more posterior faster, and more anterior slower sleep spindles (Jobert et al., 1992; Broughton and Hasan, 1995; Zeitlhofer et al., 1997; Huupponen et al., 2008). Therefore, ascertaining to what extent the chirp effect represents true frequency modulation within single sleep spindles, or sleep spindle superimposition effects, is beyond the scope of the study. However, clear spectral chirps have been previously demonstrated and qualitatively described for single epidurally recorded frontal sleep spindles in rats (Sitnikova et al., 2009). Moreover, the absolute median chirp rate obtained here (0.3–0.4 Hz/s) lies well below the difference expected from the superimposition of fast and slow spindles (with a frequency difference around 1–2 Hz), considering a sleep spin-

dle duration between 0.5 Hz and 2 Hz. There is evidence from magnetoencephalography, functional brain imaging and electrophysiological depth studies (Werth et al., 1997; Anderer et al., 2001; Schabus et al., 2007; Dehgani et al., 2011) indicating sleep spindle temporospatial frequency variation may result from activation of differential intracranial sources, with faster, more parietal spindles often preceding and being partially superimposed with slower frontal spindles (Werth et al., 1997; Zygierevic et al., 1999; Dehgani et al., 2011). A detailed study of the influence of scalp topography over spindle frequency also showed diffuse (central+frontal) spindles to have similar frequency in central and anterior positions, which was intermediate between that of pure central (faster) and frontal (slower) spindles (Huupponen et al., 2008). Sleep spindles are known to originate in thalamic TC-RE networks before being distributed over TC projections. Visual inspection of figures showing spindle recordings obtained from different preparations – for instance, *in vivo* depth intracellular recordings from anesthetized cats (Steriade, 2000), or *in vitro* slice preparations obtained from ferrets (von Krosigk et al., 1993) – suggests some frequency modulation may already be present at the thalamic RE level, where spindle-generating rhythmic spike bursts are superimposed on a background of slowly changing polarization. Intra-spindle frequency has been directly attributed to the durations of the hyperpolarizations in thalamocortical neurons, with longer hyperpolarizations resulting in lower frequencies (Steriade, 1993).

There are several limitations to this study, including the small number of subjects, which does not allow differential sleep stage, sleep time or clock time analysis. The use of MP for sleep spindle signal reconstruction is already known. The novelty here is to use a function dictionary suitable for linear spectral chirp description, in the context of sleep spindle characterization. This dictionary is not unique, neither is the tool expected to be optimal; it should be noticed that Matching Pursuit captures the general behavior of the signal, being robust and reliable at the statistical level. An atom fitting the required criteria is not conceptually equivalent to the spindle. In this study, 707 visual spindles were reconstructed into 984 atoms, and atom duration was inversely correlated with chirp rate, despite wide variation in Zero chirp atom duration. In other words, a proportion of spindles was decomposed into relatively shorter atoms with higher chirp rates. This possibly implies a degree of non-linear, rather than linear chirp effect, which can not be verified here due to the relatively low (128 Hz) sampling rate. The problem of spindle frequency modulation has been recently treated in (Ktonas et al., 2009) using an approach focused on AM/FM signal modelling, thereby assuming non-linear frequency variation. In that study, a function with amplitude and frequency modulation was defined, and four different methods, including MP, were used to investigate six model fitting parameters in simulated signals, as well as in a limited number of spindles obtained from dementia patients and older controls (11 spindles in each sample) with a sampling rate of 512 Hz. Particularly MP as used in that work considered sine functions as mother waveforms; MP was applied without any chirp function and frequency modulation was obtained a posteriori. Differences between patients and controls were found in the frequency modulation parameters, suggesting this variable to bear promising information in the clinical context. When observing oscillation models for TC-RE or other brain structures, the tools employed to compare measures should be consistent with the type of information that is expected to emerge from those models.

In conclusion, it was possible to systematically quantify internal frequency variation in human sleep spindles using Gabor chirplet-MP signal reconstruction. It was shown that sleep spindles contain a significant proportion of high voltage, negatively chirping elements. We suggest there is increasing evidence, including that from the present study, favoring systematic measurement of one more

spindle variable, its chirp rate or internal frequency variation. Preferential occurrence of negatively chirping spindles is consistent with the hypothesis of electrophysiological modulation of neocortical memory consolidation.

Acknowledgements

GG would like to acknowledge Profs. Drs. C. Perotoni and A. Martinotto for useful technical help with HAL PC Cluster at UCS. Dr. R. Rossatto, MD is acknowledged for help with visual SS detection. Prof. Dr. M.P. Hidalgo is acknowledged for invaluable help with subject data collection. The authors wish to thank the anonymous reviewers for their very constructive comments.

References

- Anderer P, Klösch G, Gruber G, Trenker E, Pascual-Marqui RD, Zeithofer J, et al. Low resolution brain electromagnetic tomography revealed simultaneously active frontal and parietal sleep spindle sources in the human cortex. *Neuroscience* 2001;103:581–92.
- Baraniuk R, Jones D. Shear madness: new orthonormal bases and frames using chirp functions. *IEEE Transactions on Signal Processing* 1993;41(12):3543–9.
- Bodisz R, Körmendi J, Rigó P, Lázár AS. The individual adjustment method of sleep spindle analysis: methodological improvements and roots in the fingerprint paradigm. *Journal of Neuroscience Methods* 2009;178:205–13.
- Born J, Rasch B, Gais S. Sleep to remember. *The Neuroscientist* 2006;12(5):410–24.
- Broughton R, Hasan J. Quantitative topographic electroencephalographic mapping during drowsiness and sleep onset. *Journal of Clinical Neurophysiology* 1995;12:372–86.
- Buzsáki G. Memory consolidation during sleep: a neurophysiological perspective. *Journal of Sleep Research* 1998;7:17–23.
- Cui J, Wong W, Mann S. Time–frequency analysis of visual evoked potentials by means of matching pursuit with chirplet atoms. *Proceedings of the 26th Annual International Conference of the IEEE EMBS* 2004;1:267–70.
- De Gennaro L, Ferrara M. Sleep spindles: an overview. *Sleep Medicine Reviews* 2003;7:423–40.
- Dehgani N, Cash SS, Halgren E. Topographical frequency dynamics within EEG and MEG sleep spindles. *Clinical Neurophysiology* 2011;122(2):229–35.
- Destexhe A, Contreras D, Sejnowski TJ, Steriade M. A model of spindle rhythmicity in the isolated thalamic reticular nucleus. *Journal of Neurophysiology* 1994;72(2):803–18.
- Destexhe A, Sejnowski TJ. Sleep and sleep states: thalamic regulation. In: Larry R Squire, editor. *Encyclopedia of Neuroscience*. Oxford: Academic Press; 2009. pp. 973–976.
- Durka PJ, Blinowska KJ. Matching pursuit parametrization of sleep spindles. In: *Proceedings of the 18th Annual International Conference of the IEEE* 3; 1996. p. 1011–2.
- Durka PJ, Ircha D, Blinowska KJ. Stochastic time–frequency dictionaries for matching pursuit. *IEEE Transactions on Signal Processing* 2001;49(3):507–10.
- Durka PJ, Szeltenberger W, Blinowska KJ, Androsiuk W, Myszka M. Adaptive time–frequency parametrization in pharmaco EEG. *Journal of Neuroscience Methods* 2002;117:65–71.
- Gribonval R. Fast matching pursuit with a multiscale dictionary of Gaussian chirps. *IEEE Transactions on Signal Processing* 2001;49:994–1001.
- Huupponen E, Väri A, Himanen SL, Hasan J, Lehtokangas M, Saarinen J. Optimization of sigma amplitude threshold in sleep spindle detection. *Journal of Sleep Research* 2000;9:327–34.
- Huupponen E, Gómez-Herrero G, Saastamoinen A, Väri A, Hasan J, Himanen SL. Development and comparison of four sleep spindle detection methods. *Artificial Intelligence in Medicine* 2007;40:157–70.
- Huupponen E, Kulkas A, Tenhunen M, Saastamoinen A, Hasan J, Himanen SL. Diffuse sleep spindles show similar frequency in central and frontopolar positions. *Journal of Neuroscience Methods* 2008;172:54–9.
- Iber C, Ancoli-Israel S S, Chesson S A L, Jr, Quan S S F., for the American Academy of Sleep Medicine. *The AASM manual for the scoring of sleep and associated events: rules, terminology and technical specifications*. 1st ed. Westchester, Illinois: American Academy of Sleep Medicine; 2007.
- Jankel WR, Niedermeyer E. Sleep spindles. *Journal of Clinical Neurophysiology* 1985;2(1):1–35.
- Jobert M, Poiseau E, Jähnig P, Schulz H, Kubicki S. Topographic analysis of sleep spindle activity. *Neuropsychobiology* 1992;26:210–7.
- Ktonas PY, Golemati S, Xanthopoulos P, Sakkalis V, Ortigueira MD, Tsekou H, et al. Time–frequency analysis methods to quantify the time-varying microstructure of sleep EEG spindles: possibility for dementia biomarkers? *Journal of Neuroscience Methods* 2009;185:133–42.
- Lopes da Silva F. E.E.G analysis: theory and practice. In: Niedermeyer E, Lopes da Silva F, editors. *Electroencephalography: basic principles, clinical applications and related fields*. 5th ed. Baltimore: Lippincott Williams & Wilkins; 2005a [chapter 58].
- Lopes da Silva F. Computer-assisted EEG diagnosis: pattern recognition and brain mapping. In: Niedermeyer E, Lopes da Silva F, editors. *Electroencephalography*

- phy: basic principles, clinical applications and related fields. 5th ed. Baltimore: Lippincott Williams & Wilkins; 2005b [chapter 59].
- Mallat S. A wavelet tour of signal processing. 2nd ed. San Diego, California: Academic Press; 1999.
- Mallat SG, Zhang Z. Matching pursuits with time–frequency dictionaries. *IEEE Transactions on Signal Processing* 1993;41(12):3397–415.
- Mann S, Haykin S. The chirplet transform: physical considerations. *IEEE Transactions on Signal Processing* 1995;43(11):2745–61.
- Molaei-Ardekani B, Benquet P, Bartolomei F, Wendling F. Computational modeling of high-frequency oscillations at the onset of neocortical partial seizures: from 'altered structure' to 'dysfunction'. *NeuroImage* 2010;52:1109–22.
- Nishida M, Walker M. Daytime naps, motor memory consolidation and regionally specific sleep spindles. *PLoS ONE* 2007;4 (e341):1–7.
- Ray LB, Fogel SM, Smith CT, Peters KR. Validating an automated sleep spindle detection algorithm using an individualized approach. *Journal of Sleep Research* 2010;19:374–8.
- Rechtschaffen A, Kales A. A manual of standardized terminology, techniques and scoring systems for sleep stages in human subjects. Washington: US Government Printing Office; 1968.
- Schabus M, Dang-Vu TT, Albouy G, Balteau E, Boly M, Carrier J, et al. Hemodynamic cerebral correlates of sleep spindles during human non-rapid eye movement sleep. *PNAS* 2007;104:13164–9.
- Schiff SJ, Colella D, Jacyna GM, Hughes E, Creekmore JW, Marshall A, et al. Brain chirps: spectrographic signatures of epileptic seizures. *Clinical Neurophysiology* 2000;111:953–8.
- Schönwald SV, Gerhardt GJL, Santa-Helena EL, Chaves MLF. Characteristics of human EEG sleep spindles assessed by gabor transform. *Physica A* 2003;327:180–4.
- Schönwald SV, de Santa-Helena EL, Rossatto R, Chaves ML, Gerhardt GJL. Benchmarking matching pursuit to find sleep spindles. *Journal of Neuroscience Methods* 2006;156(1–2):314–21.
- Sitnikova E, Hramov AE, Koronovsky AA, van Luijtelar G. Sleep spindles and spike-wave discharges in EEG: their generic features, similarities and distinctions disclosed with Fourier transform and continuous wavelet analysis. *Journal of Neuroscience Methods* 2009;180:304–16.
- Steriade M. Corticothalamic resonance states of vigilance and mentation. *Neuroscience* 2000;101(2):243–76.
- Steriade M. Cellular substrates of brain rhythms. In: Niedermeyer E, Lopes da Silva F, editors. *Electroencephalography: basic principles, clinical applications and related fields*. 3rd ed. Baltimore: Williams & Wilkins; 1993. p. 27–62, chapter 3.
- Steriade M. Brain electrical activity and sensory processing during waking and sleep states. In: Kryger MH, Roth T, Dement WC, editors. *Principles and practice of sleep medicine*. 4th ed. Philadelphia: PA: Elsevier Saunders; 2005. p. 101–19 [Ch9].
- Talakoub O, Cui J, Wong W. Approximating the time–frequency representation of biosignals with chirplets. *EURASIP Journal on Advances in Signal Processing* 2010:1–10.
- von Krosigk M, Bal T, McCormick DA. Cellular mechanisms of a synchronized oscillation in the thalamus. *Science* 1993;261:361–4.
- Werth E, Achermann P, Dijk D-J, Borbély A. Spindle frequency activity in the sleep EEG: individual differences and topographic distribution. *Electroencephalography and Clinical Neurophysiology* 1997;103:535–42.
- Yin Q, Qian S, Feng A. A fast refinement for adaptive Gaussian chirplet decomposition. *IEEE Transactions on Signal Processing* 2002;50(6):1298–306.
- Zeitlhofer J, Gruber G, Anderer P, Asenbaum S, Schimicek P, Saletu B. Topographic distribution of sleep spindles in young healthy subjects. *Journal of Sleep Research* 1997;6:149–55.
- Zygierevicz J, Blinowska KJ, Durka PJ, Szelenberger W, Niemcewicz S, Androsiuk W. High resolution study of sleep spindles. *Clinical Neurophysiology* 1999;110:2136–47.